Journal of Ovonic Research Vol. 5, No. 4, August 2009, p. 107 - 116

SYNTHESIS AND CHARACTERIZATION OF Mn^{2+} -DOPED ZnS LUMINESCENT NANOCRYSTALS

G.Murugadoss*, B.Rajamannan, V. Ramasamy, G.Viruthagiri.
Department of Physics, Annamalai University, Annamalai nagar 608 002, Tamilnadu, India

The monodisperse of the undoped ZnS and Mn^{2+} -doped ZnS nanoparticles were synthesized through chemical precipitation method using a high-boiling solvent. The prepared nanostructures of the particles have been analyzed by X-ray diffraction (XRD), scanning electron microscope (SEM), transmission electron microscope (TEM), UV-vis spectrometer and photoluminescence (PL) techniques. The size of the particles is found to be 3-5 nm range. The Mn^{2+}-doped ZnS nanoparticles dispersed in ethylene glycol (EG) shows the PL emission in the visible region 400-650 nm under UV excitation.

(Received August 1, 2009; Accepted August 25, 2009)

Keywords: Nanoparticles; Photoluminescence; XRD; TEM; Band gap.

1. Introduction

In recent times there have been extensive studies on luminescent semiconductor nanocrystals because of their potential applications in future optoelectronic devices. The nanosized semiconductor crystallites could change optical properties which are different from bulk materials [1-4]. This is the so-called quantum confinement that is observed as a blue-shift in absorption spectra with a decrease of particle size [5]. As the size is reduced to approach the exciton Bohr radius, there are some drastic changes in the electronic structure and physical properties, for example, a shift to higher energy, the development of discrete features in the spectra and concentration of the oscillator strength into just a few transitions [6], the electronic state is the limiting three-dimensional confinement which leads to molecular orbit (strong confinement) [6], surface effects, and geometrical confinement of phonons. Therefore, it has stimulated great interest in both basic and applied research [4].

Generally, ZnS becomes good host material, since it is a kind of wide band gap II-VI component semiconductor materials (E_g ~ 3.6 eV), and with its energy band characteristics. It is commercially used as a phosphor and thin-film electroluminescence devices [7, 8]. Luminescence characteristic of impurity-activated ZnS nanocrystals differ markedly from those of bulk ZnS. Yang et al. [9] give two reasons for this behavior: First, ZnS nanocrystallites are the high disperse nanocrystalline system; second, the size-dependant properties of semiconductor ZnS nanoparticles are particularly interesting. It is well-known that the properties of pure ZnS nanoparticles are obviously different from the bulk materials, nanocrystals doped with optically active luminescence centers create new opportunities for luminescent study and application of nanosemiconductor materials [10, 11].

Particularly, Mn^{2+} doped ZnS nanoparticles are widely recognized as an efficient phosphor, especially, when it is used as a phosphor material for electroluminescent displays [12]. Therefore, Mn^{2+}-doped nanocrystals have attracted much attention in recent years [13-18]. Nanosized and thus optically transparent emitters for electroluminescent displays made by simple

*Corresponding author: murugadoss_g@yahoo.com

thick film technologies (e.g., printing) would offer exciting new capabilities for industrial application of these nanomaterials in lamps or displays.

Mn^{2+} doped ZnS particles can be obtained in many ways, e.g., a spray-based method [19], mechnochemical route [20], coating method [21], synthesis by γ- irradiation of solution [22], and chemical reaction method [13,23]. The present work reports, the PL characteristics of Mn^{2+} doped ZnS nanoparticles, synthesized by chemical pricipitation method. It is the most popular technique that is used in industrial applications because of its cheap raw materials, easy handling and large-scale production [24]. The monodisperse ZnS and ZnS:Mn^{2+} nanoparticles were prepared using a high-boiling solvent (EG).

2. Experimental

ZnS with doped Mn^{2+} nanoparticles were synthesized through the chemical precipitation method using ethylene glycol as a solvent. The solvent used in the experiments was the mixture of deionized water and with different amount (10, 20 30 40 50and 60 ml) of Ethylene Glycol (EG). First, a desired molar proportion of $ZnSO_4 \cdot 7H_2O$ and $MnCl_2 \cdot 4H_2O$ were dissolved in the mixed medium of deionized water and EG. Then, the water/EG solution of Na_2S was added dropwise by an addition to the above mixture solution. During the whole reaction process, the reactants were vigorously stirred at 160˚C. To obtain powder samples, the resulting nanoparticles were cleaned repeatedly with deionized water and methanol. Finally, the powder dries at 60˚C under vacuum for two hours.

The X-ray diffraction (XRD) patterns of the ZnS and ZnS:Mn^{2+} samples were recorded using XPERT-PRO diffractometer with a Cu Kα radiation (λ=1.54060 Å) under the same conditions. The crystallite size was estimated using the Scherer equation $(0.9\lambda)/ (\beta \cos\theta)$ at the half-width at a half-maximum of the major XRD peak. The optical transmission/absorption spectra of the same particles in de-ionized water were recorded using UV-1650PC SHIMADZU spectrometer. The size and morphology of the composite particles were determined using TEM (PHILIPS-CM200; 20-200kV) and scanning electron microscopy (SEM; JEOL-JSM-5610 LV). For sample preparation, dilute drops of suspension were allowed to dry slowly on carbon-coated copper grids for TEM and on a carbon wafer for SEM measurements. Elemental composition was analyzed using EDX attachment in the same SEM instrument. Fluorescence measurements were performed on a RF-5301PC spectrophotometer. Emission (350-700 nm) spectra were recorded under 315 nm excitation for the all samples.

3. Results and discussion

The Fig. 1 shows the UV-vis spectra of Mn^{2+} -doped ZnS. As seen in the figure 1, the absorption edges of both samples were appeared at around 315 nm, which is fairly blue-shifted from the absorption edge at 345 nm of the bulk ZnS [25]. Generally, semiconductor crystallites in the diameter range of few nanometers show a quantum size effect in their electronic structure. These quantum size effects on the band gap absorption energy can be measured by UV-vis absorption spectroscopy.

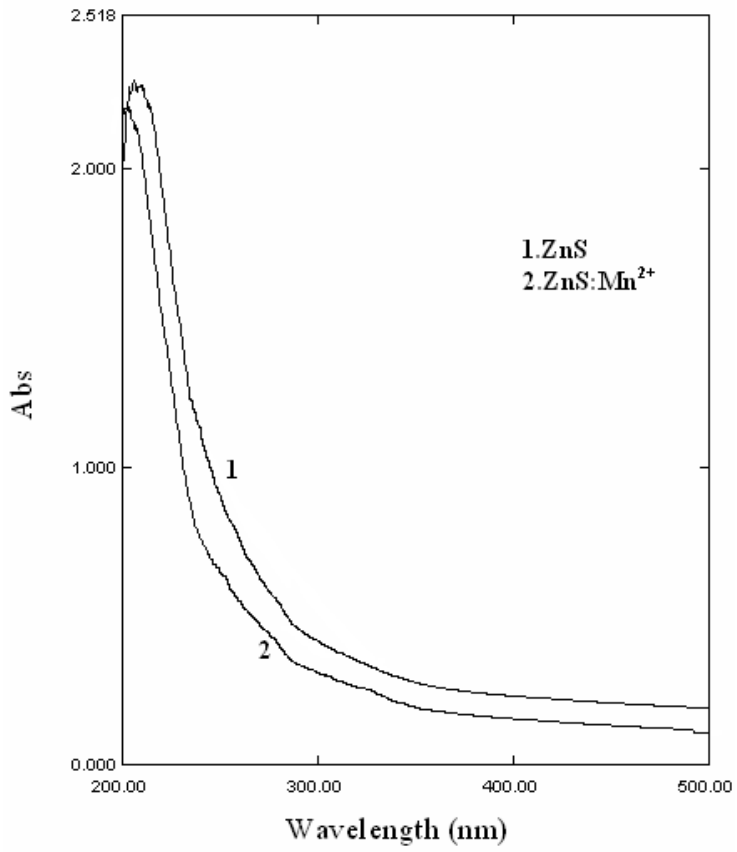

Fig. 1. Absorption spectra of Mn^{2+} doped ZnS nanoparticles.

From this study one can calculate the energy band gap. The fundamental absorption, corresponds to the transmission from valence band to conduction band, is employed to determine the band gap of the material. From figure. 1, the absorption coefficients (α) were calculated. The relation between absorption coefficient (α) and incident photon energy (hν) can be written as

$$\alpha = A\,(h\nu - E_g)^n / h\nu$$

Where A is a constant and E_g is the band gap of the material.

Exponent "n" depends upon the type of the transition; n may have values 1/2, 2, 3/2 and 3 corresponding to the allowed direct, allowed indirect, forbidden direct and forbidden indirect respectively [26]. In the nanocrystalline sample, the transition is same as in the case of bulk. However there may be some deviation from the bulk. From the above equation, it is clear that, plot of $(\alpha h\nu)^2$ versus hν will indicate a divergence of an energy value, E_g where the transition takes place.

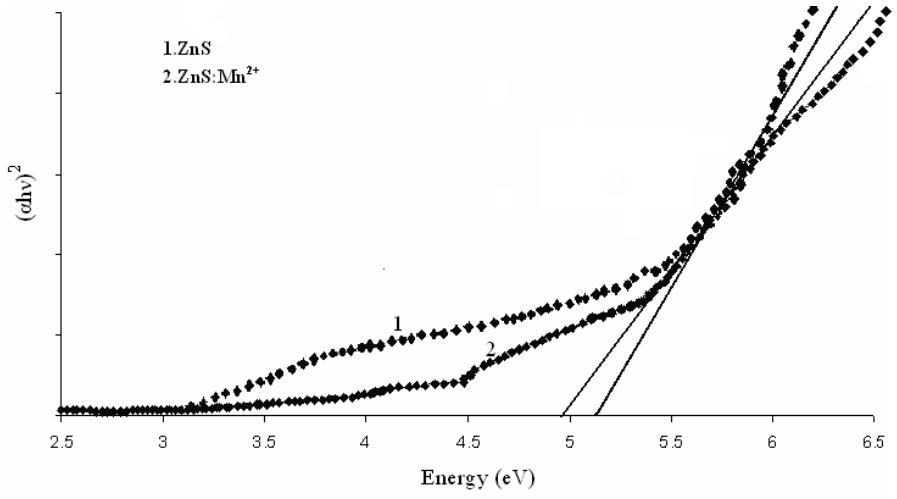

Fig. 2. hν vs. $(\alpha h\nu)^2$ of the samples.

The exact value of the band gap is determined by extrapolating the straight line portion (Fig. 2) of $(\alpha h\nu)^2$ versus hν. The calculated band gap values are 5.15eV for ZnS and 4.9eV for ZnS:Mn^{2+} nanoparticles. It is noticed that the band gap value is higher than the bulk value (3.6eV) of ZnS. From the band gap values, the particles sizes were calculated [24] from the following formula:

$$E_{gn} = [E^2_{gb} + \{2h^2 E_{gb} (\pi/R)^2/m^*\}]^{1/2} ,$$

Where R is the radius of the quantum size particles (i.e. nano particles), E_{gn} and E_{gb} are the band gap of nano and bulk systems, respectively and m* is the effective electron mass (m* = $0.22m_e$). The particle size of nano ZnS from this equation is 8.5 nm and 9.2 nm for ZnS: Mn^{2+}. The average particles sizes of the nano ZnS and ZnS: Mn^{2+} from this equation are agreed quite well the particle size estimated through XRD (3.8 and 4.2 nm for ZnS and ZnS: Mn^{2+} respectively). Bhargava et al [27, 28] reported that, if the particle size is decreased, a strong hybridization of the s-p states of the ZnS host and the d states of the Mn^{2+} impurity should occur.

Fig. 3 shows the X-ray powder diffractogram of nanocrystalline ZnS and ZnS: Mn^{2+} prepared with 50 ml of EG was used as a solvent. It is revealed that these nanoparticles having zinc blende structure with planes at (111), (220) and (311), respectively. The XRD peaks are broadened due to the nanocrystalline nature of particles. These nanocrystals have lesser lattice planes compared to bulk, which contributes to the broadening of the peaks in the diffraction pattern. This broadening of the peak could also arise due to the micro-straining of the crystal structure arising from defects like dislocation and twinning etc. These defects are believed to be associated with the chemically synthesized nanocrystals as they grow spontaneously during chemical reaction. As a result the chemical ligands get negligible time to diffuse to an energetically favorable site. It could also arise due to lack of sufficient energy needed by an atom to move to a proper site in forming the crystallite.

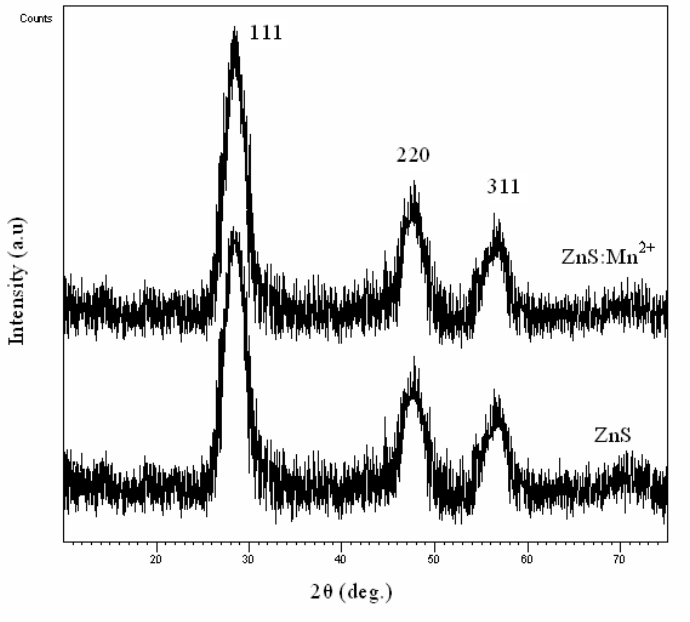

Fig. 3. XRD pattern of ZnS and ZnS:Mn^{2+} nanoparticles

From the value of FWHM, the mean crystalline sizes were calculated using Scherer's equation ($D = 0.9\lambda/ (\beta \cos\theta)$), where λ is the X-ray wavelength, θ is the diffraction angle and β is the full with half maximum of the particles. The calculated mean crystal size is 3.8 nm for ZnS and 4.2 nm for ZnS:Mn^{2+} .

As observed in the experiments, nanoparticles were made within the first few minutes, but after a few minutes, those particles were aggregated and their size become larger, because of their large surface to volume ratio. In fact, without coating of surfactant on the particles, due to the increase in the surface area to volume ratio, the attractive force between the nanoparticles will increase, and the particles will agglomerate. Thus, the particle size becomes larger (see Fig. 4a & 4b).

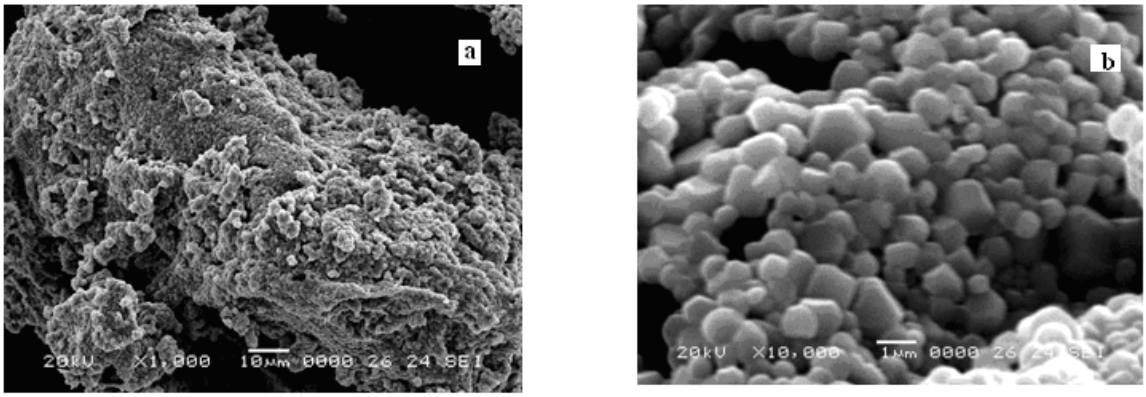

Fig. 4. SEM micrograph of ZnS:Mn^{2+} nanoparticles without EG.

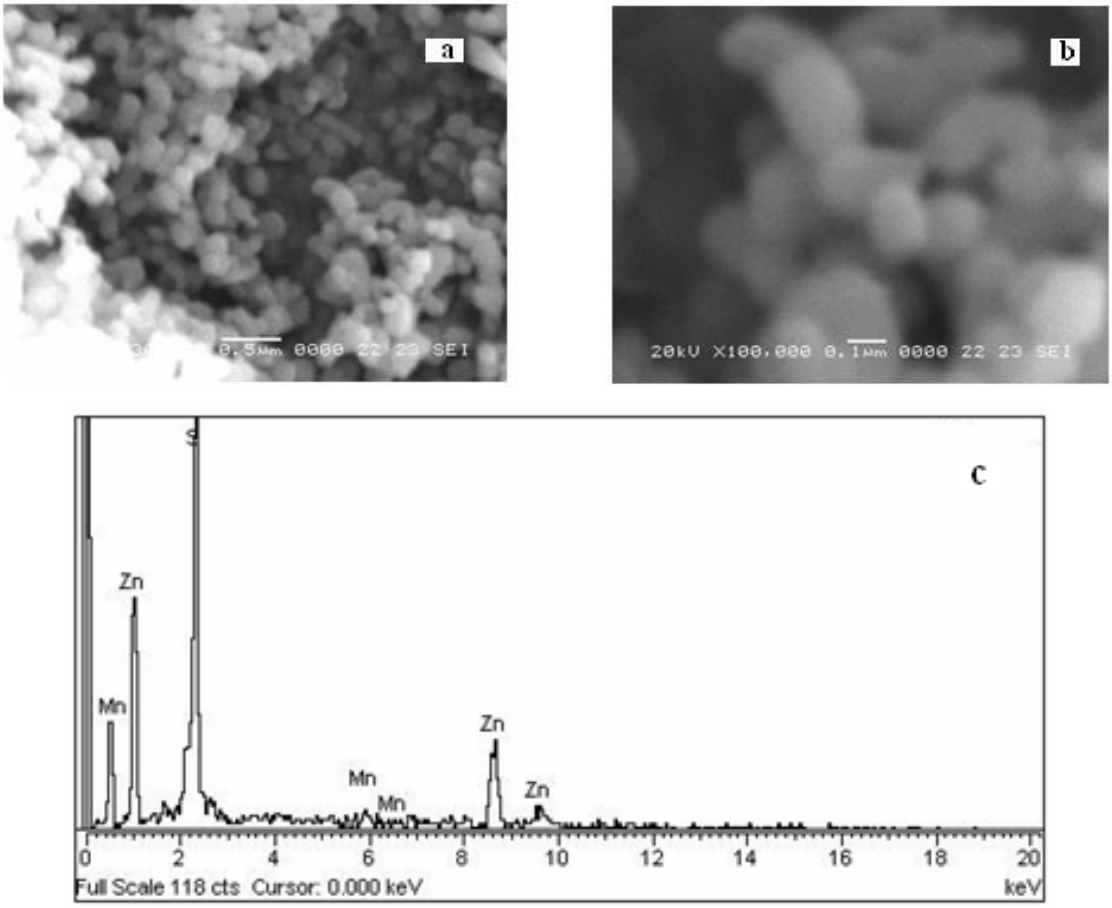

Fig. 5. SEM micrograph of ZnS:Mn^{2+} nanoparticles at (a) low magnification, (b) high magnification with EG and (c) EDX spectrum of the sample.

To overcome this problem, EG is used during the preparation, which acts as a barrier for the fast movement of solutes due to its viscous nature. In this case, a significant amount of EG may be loosely-bound paint on the individual particle surface which could perform as nano-scaled reactors.

SEM allows imaging of individual crystallites and the development of a statistical description of the size and shape of the particles in a sample. Fig. 5(a) and 5(b) show the SEM images of synthesized Mn^{2+} doped ZnS nanoparticles using ethylene glycol as a solvent. These nanoparticles are in spherical shape and show an average agglomerate size, only below 50 nm since it is limited by the resolution. However, an actual particle size calculated through X-ray diffraction is below 5 nm. The elemental composition determined through EDX attached with SEM instrument is shown Fig. 5(c). This reveals that the Mn^{2+} ions are incorporated in the Zn^{2+} lattice sites.

Fig. 6(a) and (b) display a representative TEM images of ZnS:Mn^{2+} nanoparticles and Fig. 6(c) corresponds to electron diffraction pattern. These nanoparticles are nearly spherical and have an average particle size of about 5 nm, which is in good agreement with the value obtained from XRD analysis. The lattice fringes can be observed in the TEM image. As shown in Fig. 6(c), the electron diffraction pattern consists of three concentric sharp rings, which correspond to (111), (220), and (311) diffraction of the cubic structure. Therefore, it can be further confirmed that the nanoparticles are in the cubic zinc blende structure.

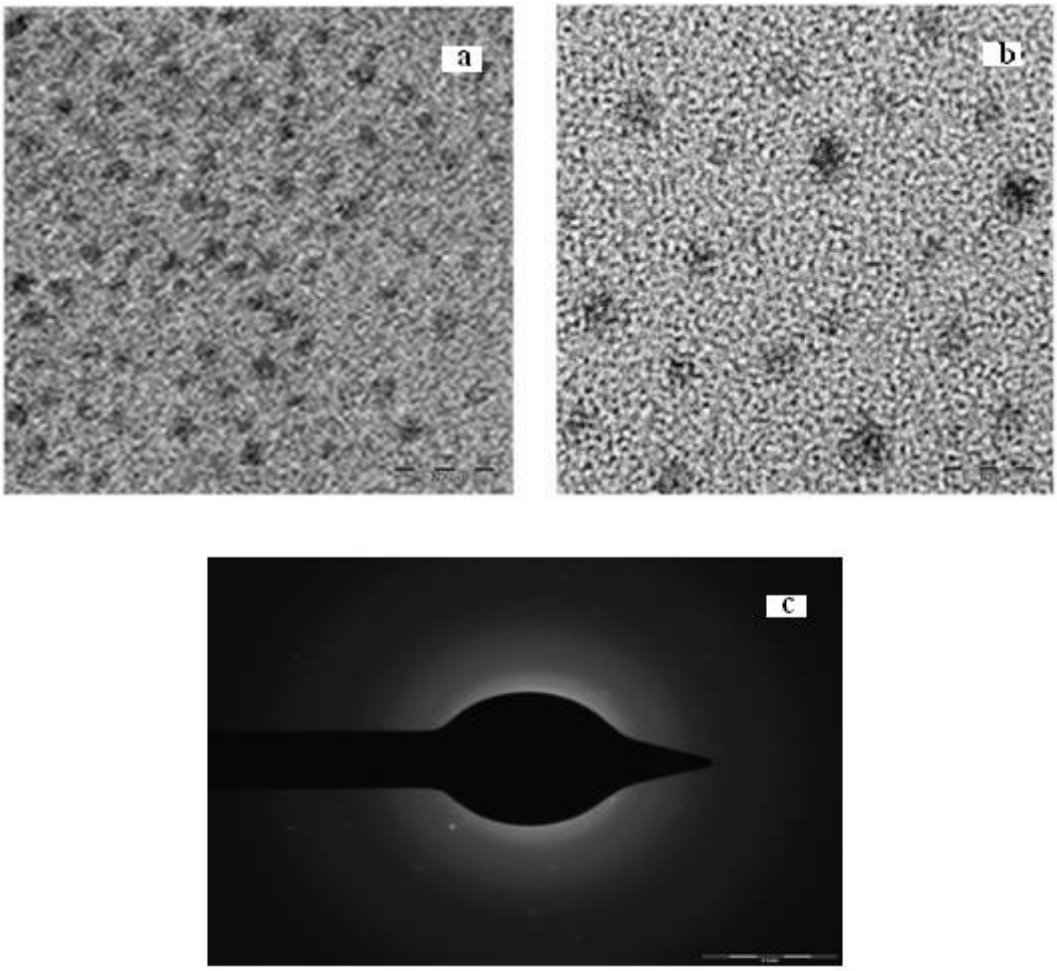

Fig. 6(a) and (b). Transmission Electron Microscope images of the Mn^{2+} doped ZnS nanoparticles. The scale bar represents 20 nm (c) Electron diffraction image of the same particles.

The PL spectra of the undoped ZnS and doped ZnS:Mn^{2+} nanoparticles are demonstrated in Fig. 7. It was found that the emission intensity is large when the excitation wavelength was 315 nm for both samples. The emission band from the undoped ZnS nanoparticles is highly symmetric and broad. This broadening indicates the involvement of single luminescence center in the radiative process in visible range (blue emission) and symmetric nature indicates monodisperse of particles in the prepared solution. The peak photoemission takes place at 445 nm which could be ascribed to a recombination of electrons at the sulfur vacancy donor level with holes trapped at the zinc vacancy acceptor level.

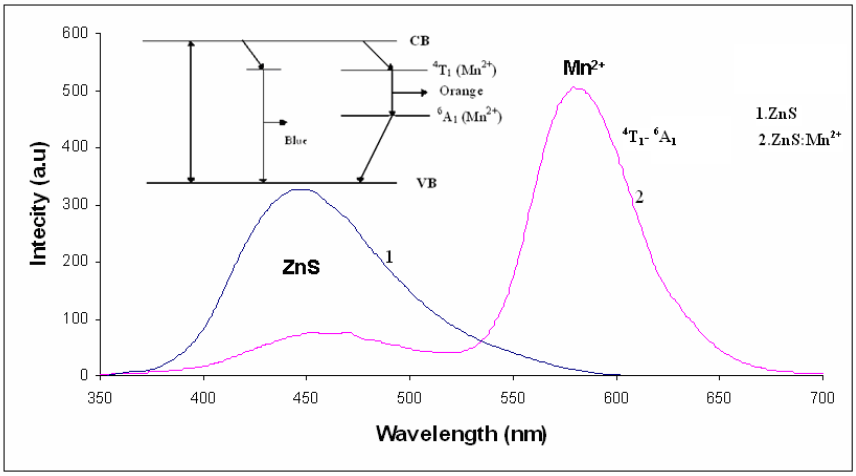

Fig. 7. The room temperature PL spectra of ZnS and ZnS:Mn^{2+} showing the emission peaks are at 445 for undoped ZnS and 581 nm for Mn (4%) doped ZnS under 310 nm excitation. The recombination mechanism for the ZnS:Mn^{2+} system shows in inset of the figure.

The addition of EG in the experimental process seems to play a key role in obtaining the highly monodisperse ZnS nanocrystals. It is obviously seen in SEM (Fig. 5a&5b) and TEM (Fig. 6a&6b) micrographs. The formation mechanism of monodisperse particles originally proposed by LaMer and Dinegar [29], the growth rate depends mainly on three factors, namely, the number of nuclei which are to grow, the total amount of diffusible nuclei, and their diffusion coefficient in the medium. It is obvious that the diffusion depends inversely on the viscosity of the reaction medium. In the present synthetic procedure, the addition of EG in the solution does not have any effect on the first two factors but has an obvious effect on the viscosity of the reaction medium due to increasing of concentration. This promoted the homogeneous growth of the crystal nuclei and finally the formation of monodisperse nanocrystals. These similar results were also been reported by Li [30] for the formation of monodisperse Bi_2O_3 nanocrystals using high viscous poly ethylene glycol with proper molecular weight. In the present work, when the amount of EG is increased from 10 to 50 ml, the intensity of both, blue (445 nm) and yellow-orange (581 nm) emissions (Fig. 8.) are increased due to monodisperse of the particles. Further increase of EG (60 ml) in the reaction medium decreases the emission intensity of the yelloe-orange emission (inset of the Fig. 8). It may be due to reduction of growth rate (nanocrystals) by the way of resisting the diffusion in increasing viscosity. Thus it is observed that EG plays dual role in the prepared solution as solvent and as barrier for the fast movement of the growth nuclei.

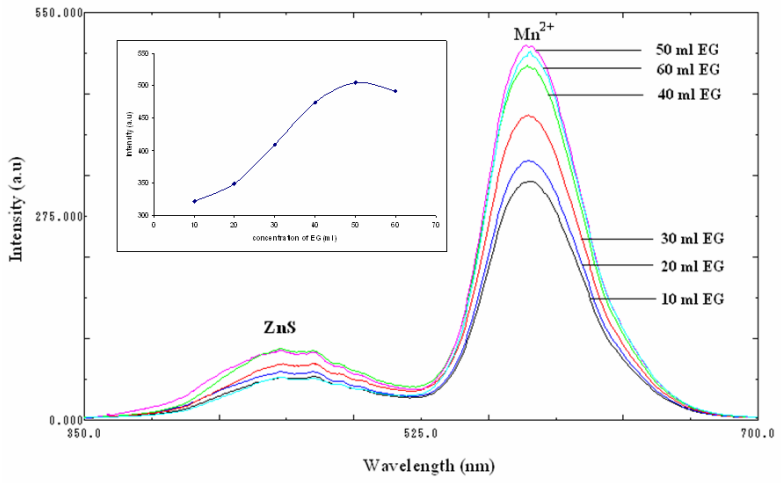

Fig. 8. The room temperature PL spectra of ZnS:Mn^{2+} nanoparicles with different amount of EG (10 – 60 ml).

Peng et al [31] analyzed the PL spectra of ZnS:Mn^{2+} nanoparticles and monitored the characteristic orange emission of Mn^{2+} at 600 nm. Bhattacharjee et al [32] recorded the PL spectrum of ZnS:Mn^{2+} particles at room temperature using chemical precipitation method. It reveals broad blue emission signal centered at ~420 nm and Mn^{2+} related yellow-orange band centered at ~590 nm. Recently, Qi Xiao and Chong Xiao [33] reported the peak intensity at 585 nm for the same particles using the same chemical method. However, the emission spectrum of Mn^{2+} doped with ZnS particles of the present study shows blue shift of the yellow-orange emission peak at 581 nm. The orange photoluminescence originate from a transition between the $^4T_1$ excited state and the $^6A_1$ ground state of the Mn^{2+} ion within a nanocrystalline ZnS lattice. Due to the small particle size in 4.2 nm, surface defects such as donors and acceptors are easily formed on the ZnS nanocrystals surface. When an electron is prompted to the excited state, there are two main paths for the electron to relax to the ground state. One is the relaxation process through surface defects, such as donor and acceptors. This relaxation will usually give rise to a non-radiative recombination and/or light emission by other wavelengths. The other emission is due to an intraconfigurational $3d^5$ transition on the Mn^{2+} ion located within the band gap of ZnS nanocrystals. This $^4T_1$-$^6A_1$ energy transition gives rise to an orange photoluminescence. The large linewidth of the yellow-orange emission is due to a combination of inhomogeneous broadening and phonon assisted transition [27].

4. Conclusion

ZnS:Mn^{2+} nanoparticles with distinguishable morphology were synthesized through chemical precipitation method using high boiling solvent. The addition of EG more than 50 ml causes decrease in emission intensity. The particles exhibited the characteristic yellow-orange emission (excited at 315 nm) centred at 581 nm for Mn^{2+} ions. Convoluted PL spectrum of nanoparticles suggested that there is a blue shifted in the above emission.

Acknowledgements

The authors thank to Dr. AN. Kannapan, Professor and Head, Department of Physics, Annamalai University for providing lab facilities

References

[1] L. E. Brus, J. Phys. Chem. **90,** 2555 (1998).
[2] R. Rossetti, R. Hull, T. M. Gibson, L. E. Brus, J. Chem. Phys. **82,** 552 (1985).
[3] A. P. Alivisatos, J. Phys. Chem. **100,**13226 (1996).
[4] R. Pool, Science **248,** 1186 (1990).
[5] Z. L. Wang et al. (Eds.), Tsinghua University Press and Kluwer Academic/Plenum Publishers, (2002).
[6] Handbook of Nanostructured Materials and Nanotechnology, Hari Singh Nalwa (Ed.), Optical Properties, vol. 4, Academic Press, (2000).
[7] I. P. McClean, C. B. Thomas, Sci. Technol. **7,** 1394 (1992).
[8] I. Yu, M. Senna, Appl. Phys. Lett. **66,** 424 (1995).
[9] P. Yang, M. K. Lu, D. R. Yuan, C. F. Song, S. W. Liu, X. F. Cheng, J. Opt. Mater. **24,** 497 (2003).
[10] R. N. Bhargava, D. Gallagher, T. Welker, J. Lumin. **60,** 275 (1994).
[11] Y. Yi, Y. Ding, Y. Zhang, Y. Qian, J. Phys. Chem. Sol. **60,** 13 (1993).
[12] J. K. Furdyna, J. Appl. Phys. **64**, R29 (1988).
[13] H. Yang, P. H. Hollowy, and B. B. Ratna, J. Appl. Phys. **93,** 586 (2003).
[14] S. C. Erwin, L. Zu, M. I. Haftel, A. L. Efros, T. A. Kennedy, and D. J. Norris, Nature. **436,** 91 (2005).

[15] A. A. Bol and A. Meijerink, J. Phys. Chem. B. **105,** 10197 (2001).
[16] F. H. Su, Z. L. Fang, B. S. Ma, K. Ding, G. H. Li, and W. Chen, J. Phys. Chem.. **107 B**, 6991 (2003).
[17] N. Karar, F. Singh, and B. R. Mehta, J. Appl. Phys. **95,** 915 (2004).
[18] S. Sapara, A. Prakash, A. Ghangrekar, N. Periasamy, and D. D. Sarma, J. Phys. Chem. **109B,** 1663 (2005).
[19] L. Amirav, A. Amirav, E. Lifshitz, J. Phys. Chem. **109 B,** 9857 (2005).
[20] P. Balaz, E. Boldizarova, E. Godocikova, J. Briancin, J. Mat. Lett. **57,** 1585 (2003).
[21] II. Yu, Tetsuhiko Isobe, Mamoru Senna, and Shin-ichi Takahashi, Mater. Sci. and Eng. **38 B**, 177 (1996).
[22] A. H. Souici, N. Keghouche, J. A. Delaire, H. Remita, M. Mostafavi, Chem. Phys. Lett. **422,** 25 (2006).
[23] J. H. Chung, C .S. Ah, D. J. Jang, J. Phys. Chem. **105 B,** 4128 (2001).
[24] Z. L. Wang. Et al. (Eds), Handbook of Nanophase and Nanostructured Materials - Synthesis, Tsinghua University Press and Kluwer Academic/Plenum Publishers, (2002).
[25] P. Vinotha Boorana Lakshmi, K. Sakthi Raj, K. Ramachandran, Cryst. Res. Technol. **44,** 153 (2009).
[26] J. I. Pankove, Optical Processes in Semiconductor (Prentice-Hall, New Jersey, (1971).
[27] R. N. Bhargava, D. Gallagher, X. Hong, A. Numikko, Phys. Rev. Lett. **72,** 416 (1994).
[28] M. Boshta, S. A. Gad, A. M. Abo El-Soud, M. Z. Mostafaa, J. Ovonic Research, **4** 175 (2008)
[29] V. K. La Mer, R. H. Dinegar, J. Am. Chem. Soc**.72,** 4847 (1950).
[30] Li, W. Mater. Chem. Phys. **99,** (2006)174.
[31] W. Q. Peng, S.C. Qu, G. W. Cong , X. Q. Zhang and Z. G. Wang, ,J. Cryst. Growth. **282,** 179 (2005).
[32] Bhattacharjee, D. Ganguli, K. Iakoubovskii, A. Stesmans and S. Chaudhuri, Bull. Mater. Sci. **25,** 175 (2002).
[33] Q. Xiao, C. Xiao, Appl. Phys. Sci. **254,** 6432 (2008).